DOE/PC/90012-8

Hydrodynamics of Three-Phase Slurry Fischer-Tropsch Bubble Column Reactors

Quarterly Technical Progress Report

for the Period 1 April 1989 - 30 June 1989

Dragomir B. Bukur, James G. Daly and Snehal A. Patel

Texas A&M University

Department of Chemical Engineering

College Station, TX 77843

July 24, 1989

Prepared for the Pittsburgh Energy Technology Center,

the United States Department of Energy Under Contract No. DE-AC22-86PC90012

George Cinquegrane, Project Manager (PETC)

John Shen, Program Manager (DOE/FE)

DOE/PC/90012-8

Hydrodynamics of Three-Phase Slurry Fischer-Tropsch Bubble Column Reactors

Quarterly Technical Progress Report

for the Period 1 April 1989 - 30 June 1989

Dragomir B. Bukur, James G. Daly and Snehal A. Patel

Texas A&M University

Department of Chemical Engineering

College Station, TX 77843

July 24, 1989

Prepared for the Pittsburgh Energy Technology Center,

the United States Department of Energy Under Contract No. DE-AC22-86PC90012

George Cinquegrane, Project Manager (PETC)

John Shen, Program Manager (DOE/FE)

NOTICE

PATENT STATUS

TECHNICAL STATUS

TABLE OF CONTENTS

I. Abstract

During the past quarter we conducted an additional eleven hot flow experiments in the 0.05 m ID stainless steel column. Six of these were conducted using FT-300 wax as the liquid medium and the remaining five using Sasol wax. Batch and continuous mode runs were made with both waxes using large iron oxide particles. While significant solids concentration gradients were observed during the batch mode runs, the profiles during the continuous mode were either uniform (at a liquid velocity of 0.02 m/s), or showed a slight gradient (at u_l=0.005 m/s). Hold-up values with Sasol wax were lower than those due to FT-300 wax for all cases, due to the foaming tendency of the FT-300 wax. Axial dispersion coefficients were estimated for the batch mode runs with solids, and the values showed no effect of liquid type and a marginal effect of solids type (silica vs. iron oxide).

The Cesium-137 source and detector were used during the hot flow runs in the small column, and the resulting data were analyzed to obtain slug frequencies and flow regime transitions. Our results indicate that the transition occurred at about the same gas velocity for all cases, and furthermore, the slug frequency at a gas velocity of 0.09 m/s approached 2.5 Hz for all runs.

II. Objective and Scope of Work

The overall objective of this contract is to determine the effects of bubble column diameter, solids loading and particle size, and operating conditions (temperature, gas and liquid flow rates) on hydrodynamics of slurry bubble columns for Fischer–Tropsch synthesis, using a molten wax as the liquid medium. To accomplish these objectives, the following specific tasks will be undertaken.

Task 1 – Project Work Plan

The objective of this task is to establish a detailed project work plan covering the entire period of performance of the contract, including a detailed program schedule, analytical procedures, and estimated costs and manhours expended by month for each task.

Task 2 – Design and Construction of the Experimental Apparatus

The existing glass and stainless steel columns (0.051 m and 0.229 m in diameter, 3 m tall) that were constructed under our previous DOE contract (DE–AC22–84PC70027), will be modified and additions made in order to study the effect of continuous upward liquid flow. After the procurement of equipment and instrumentation, and construction of the unit is completed, a shakedown of test facilities will be made to verify achievement of planned operating conditions.

Task 3 – Measurement of Hydrodynamic Parameters by Conventional Techniques

In this task, the effects of operating conditions (liquid and gas superficial velocities, temperature), gas distributor, column diameter, and solids concentrations and particle size on hydrodynamic parameters in the glass and stainless steel columns will be determined. All experiments will be conducted using nitrogen at atmospheric pressure.

The hydrodynamic parameters that will be determined as a function of the independent variables mentioned above are: average gas hold–up, axial solids distribution, axial gas hold–up, flow regime characterization, and qualitative information on bubble size distribution.

Task 4 – Application of a Gamma Radiation Density Gauge for Determining Hydrodynamic Parameters

The objective of this task is to determine hydrodynamic parameters for the three–phase system using a nuclear density gauge apparatus. A movable assembly mechanism and positioning racks for the two nuclear density gauges and detectors will be designed and constructed. Following the interfacing of the apparatus with an on–line microprocessor, the gauges will be calibrated using pure components (liquid wax and solid particles), and with known proportions of liquid and solid. After calibration, the following parameters will be obtained from experiments in the large stainless steel column: axial gas hold–up, axial concentration of solids, and qualitative information on flow regimes and bubble size distributions.

III. Summary of Progress

Eleven hot flow experiments were made in the 0.05 m ID column during the past quarter. Gas velocities of 0.02, 0.04, 0.06 and 0.09 m/s were employed in all runs. The experiments were done at 265°C using the 2 mm orifice plate distributor. Six of the experiments were made using FT-300 wax as the liquid medium and the remaining five experiments were conducted using Sasol wax. No major operational problems were encountered during these series of experiments. The rebuilt pump from Gelber Pumps (Chicago) performed satisfactorily. Some problems with solids settling were encountered during continuous mode experiments at a liquid circulation velocity of 0.005 m/s; however, we were able to maintain solids concentrations close to the desired levels during the various runs.

During the batch mode experiment with FT-300 wax (in the absence of solids), foam was present above the dispersion till a gas velocity of 0.06 m/s. Thereafter, the layer of foam collapsed (at 0.09 m/s) and gas hold-up decreased. When a liquid circulation velocity of 0.005 m/s was introduced, hold-up values were lower than those obtained in the batch mode of operation, except at a gas velocity of 0.09 m/s (where foam had broken in the batch mode run). When 20 wt.% of 20-44 μm iron oxide was added to FT-300 wax, hold-ups increased significantly and for the batch mode run with this slurry, hold-up values were even higher than those obtained in the batch mode of operation without solids. The addition of the iron oxide particles contributed to the foaming tendency of the wax, causing the high gas hold-ups. The hold-ups were lowered by introducing liquid circulation, and at a liquid circulation velocity of 0.005 m/s, hold-ups were even lower than those observed in the continuous mode of operation without solids.

The addition of silica to FT-300 wax (20 wt.% of 20-44 μm particles), did not have a significant effect on the gas hold-up. Hold-up values from the batch mode run with

this slurry were comparable to values obtained in the batch mode run without solids.

Hold-up values with Sasol wax were less affected by the presence of solids or by the introduction of liquid circulation. However, even with this medium, the highest gas hold-ups were obtained during the batch mode of operation with a slurry containing 20 wt.% of 20-44 μm iron oxide. The hold-ups with this slurry dropped when liquid circulation was introduced.

Axial dispersion coefficients were determined for iron oxide and silica for the three runs conducted in the batch mode of operation. Hindered settling velocities were estimated using literature correlations, and used to calculate the dispersion coefficients from the U_p/Es ratios. Dispersion coefficients for the two types of solids ranged between 20 and 40 cm^2/s at most gas velocities. There was no effect of liquid medium, and the effect of solids type was marginal. Solids concentration profiles, for the batch runs, showed no effect of gas velocity.

During the past quarter we also evaluated several average hold-up correlations available in literature using data obtained during the earlier runs in the 0.05 m ID column. The constants in these correlations were evaluated using nonlinear regression, and for most correlation, the measured hold-up data were within $\pm$15% of the predicted values.

The Cesium-137 source was used to determine slug frequencies and flow regime transitions for experiments conducted in the 0.05 m ID column. Results from the different runs indicate little or no effect of liquid circulation, solids, or liquid type on the slug frequency or on the gas velocity at which the transition to slug flow took place. In general, slug frequency approached 2.5 Hz at a gas velocity of 0.09 m/s, and the transition to slug flow took place at a gas velocity of about 0.04 m/s.

IV. Detailed Description of Technical Progress

A. Task 3 – Measurement of Hydrodynamic Parameters by Conventional Techniques

A.1. Overview of Bubble Column Operations

The new lobe type positive displacement pump was received from Tuthill Corporation (Chicago) in April. This pump will be used for experiments in the large (0.23 m ID) stainless steel column, whereas the rebuilt slurry pump (from Gelber Pumps) will be used in the small column (0.05 m ID) circuit. Calibration of instruments associated with the small column circuit was completed and the column was made ready for hot flow experiments.

Preparation of the 0.23 m ID stainless steel column for hot flow experiments was initiated in June. We plan to complete the installation of the pump, and related process piping by the end of July. Instrument calibration will be done thereafter.

A.2. Experimental Results

A total of eleven experiments were conducted using Sasol wax and FT-300 wax in the 0.05 m ID column. Table 1 summarizes the conditions used in these runs. All experiments were conducted at 265°C using the 2 mm orifice plate distributor. Measurements were made at gas velocities of 0.02, 0.04, 0.06 and 0.09 m/s for all runs. This marks the completion of experiments in this column.

Six of the eleven experiments were conducted in the continuous mode of operation, whereas the remaining five were made in the batch mode. The rebuilt slurry pump performed satisfactorily during the continuous mode tests. No problems with the pump were encountered during these runs; however, at the end of the last experiment (batch mode run with large silica), cooling water, used to cool the pump's graphite seal, began to leak into the pump head. This was probably due to wear of the seal. We encountered some problems with the settling of solids in the 1" OD overflow line (between the expansion unit and the calibration chamber). The problem interfered with normal

operations during continuous mode experiments with large iron oxide (20 - 44 μm), at a liquid circulation velocity of 0.005 m/s. The overflow line was cleared by temporarily increasing the liquid circulation velocity. This problem did not occur during runs made using a liquid circulation velocity of 0.02 m/s. No other operational problems were encountered during this series of runs.

Axial gas hold-up profiles were determined for all experiments, and solids concentration profiles were determined for experiments involving solids. Axial dispersion coefficients were estimated for the three batch mode experiments where solids were used.

Average gas hold – ups

Figure 1 shows overall gas hold-up values from experiments conducted with FT-300 and Sasol waxes, in the absence of solids. Foam was produced in the batch run with FT-300 wax, and hold-up increased with increasing gas velocity up to u_g=0.06 m/s. When gas velocity was further increased to 0.09 m/s, the foam appears to have collapsed and gas hold-up dropped from 28% to 23% at u_g=0.09 m/s (indicated by the broken line in Figure 1). When the experiment with FT-300 wax was repeated in the continuous mode of operation, using a liquid circulation velocity of 0.005 m/s, hold-ups were significantly lower at gas velocities of 0.04 and 0.06 m/s (velocities at which foam was present in the batch mode of operation). However, at a gas velocity of 0.09 m/s, hold-up in the continuous mode of operation was higher than that obtained during the batch mode run (28 vs. 23%). These results are similar to those obtained during our earlier experiments with FT-300 wax (Technical Progress Report for the period April - June 1988). The experiments were then made with Sasol wax, and these results are also shown in Figure 1. Unlike FT-300 wax, Sasol wax did not have a tendency to foam. Hold-up values from the batch run with this wax are similar to those obtained when a liquid circulation velocity of 0.005 m/s was used.

The differences in hold-up values for the two waxes can be attributed to the differences in the foaming tendencies of the two media. FT-300 wax has a tendency to foam, and some of this foam dissipates when liquid circulation is introduced, lowering gas hold-up values. Sasol wax, on the other hand, is a coalescing medium that produces little or no foam, and the flow regime is not significantly affected when liquid circulation is introduced. Hold-up values for this medium are therefore similar for batch and continuous modes of operation.

The effect of solids type on average gas hold-up for FT-300 wax is shown in Figure 2. Hold-up values from experiments with iron oxide, and with silica, are compared with values obtained in the absence of solids. All three experiments were conducted in the batch mode of operation. At a gas velocity of 0.02 m/s, hold-up values for all three cases were similar. At this gas velocity homogeneous bubbly flow regime prevails and the type of solids does not have any influence on the gas hold-up. However, as gas velocity was increased, all three systems produced foam, with the highest hold-up obtained in the presence of iron oxide (u_g=0.04 m/s). Hold-ups continued to increase for the system with iron oxide, whereas foam broke for the system containing silica. In general, gas hold-ups in the presence of silica were very similar to those obtained when no solids were present, except at a gas velocity of 0.06 m/s. At this gas velocity, foam was still present in the run conducted without solids. These results show that, iron oxide is conducive to foaming, while silica either suppresses foam or has no effect on hold-up. Hold-up in the presence of iron oxide reached as high as 40% at u_g=0.09 m/s.

The effect of liquid velocity, in the presence of solids (20 wt.%, 20-44 μm iron oxide), on average gas hold-ups for FT-300 wax is shown in Figure 3. Average gas hold-up values were highest during the experiment conducted in the batch mode. As shown in Figure 2, iron oxide appears to promote foaming with this medium. When liquid circulation is introduced, the foam dissipates and the extent of dissipation depends on

the intensity of the circulation. Hold-up values were lowest when a liquid circulation velocity of 0.02 m/s was used.

Figure 4 illustrates the effect of liquid circulation on gas hold-up for runs conducted with Sasol wax. The slurry contained 20 wt.% of 20-44 μm iron oxide particles. These results show that liquid circulation does not have a significant effect on average gas hold-up with this medium. The greatest difference was at a gas velocity of 0.09 m/s, where hold-up in the batch mode was 21% while that in the continuous mode was about 26%. Hold-up was not measured at a gas velocity of 0.06 m/s in the continuous mode due to operational problems. The behavior of Sasol wax is significantly different from that of FT-300 wax primarily due to the absence of foam with Sasol wax.

The effect of particle size on average gas hold-up with Sasol wax is shown in Figure 5. Results from experiments conducted with 20 wt.% of small (0-5 μm) and large (20-44 μm) iron oxide are compared with values obtained in the absence of solids. All experiments were conducted using a liquid circulation velocity of 0.005 m/s. The addition of solids appear to cause an increase in gas hold-up. The increase is only marginal when small particles were used; however, in the presence of large iron oxide, hold-up values show a more significant increase. As was observed with FT-300 wax (Figure 2), the addition of large iron oxide causes the hold-up to increase for Sasol as well. The reasons for this are not clear at the present.

Axial solids dispersion coefficients

Axial dispersion coefficients were estimated from data obtained during the three batch mode runs in the presence of solids. Solids concentration profiles for runs conducted in the continuous mode of operation were either uniform (for small particles), or showed a slight gradient (for large particles). The theoretical background for axial dispersion coefficient estimation was given in the previous Technical Progress Report (January - March, 1989). The solids concentration profiles, axial gas hold-up profiles,

and dispersion coefficients for the batch runs are discussed here.

Figures 6 to 8 illustrate the effect of superficial gas velocity on the axial gas hold-up profiles, and on the solids concentration profiles, for runs conducted with Sasol and FT-300 waxes in the batch mode of operation. In each case, the solids concentration profiles do not show a significant trend with gas velocity. The concentration of solids is greatest towards the bottom of the column, as would be expected. Axial gas hold-up profiles indicate that hold-up increases with height along the column for all runs, with the gradients being steeper at high gas velocities. For the experiment with large iron oxide in FT-300 wax, a significant amount of foam was present at the top of the dispersion, and hold-up values in this region are as high as 70% (Figure 7a).

Using the semi-infinite dispersion model, the values for U_p/E_s (hindered settling velocity/axial dispersion coefficient) were estimated for all three runs using

$$C_s = C_s^B \exp\left[-L\overline{\Phi_\ell}\frac{U_p}{E_s}x\right] \qquad (1)$$

A derivation of Eqn. 1 was given in the previous Technical Progress Report (January-March, 1989). Regression analysis on the solids concentration vs. height data was used to estimate U_p/E_s at each gas velocity. These values are shown in Figure 9a for the three runs. The ratio is lowest for silica in FT-300 wax, whereas values for iron oxide in FT-300 wax and Sasol wax are comparable. Silica has a density that is lower than that of iron oxide (2.65 g/cc vs. 5.1 g/cc), therefore, the hindered settling velocity for silica is lower than that for iron oxide. This would cause U_p/E_s for silica to be lower than that for iron oxide, assuming similar axial dispersion coefficients. We used the correlation presented by Kato et al. (1972) to estimate the hindered settling velocities for silica and iron oxide

$$U_p = 1.33 U_T^{0.75} U_g^{0.25} \overline{\Phi_\ell}^{2.5} \qquad (2)$$

These values were then substituted in the U_p/E_s values estimated earlier, and the axial

dispersion coefficients were calculated, and are plotted in Figure 9b. The dispersion coefficients for iron oxide in FT-300 wax and in Sasol wax are similar at all gas velocities. Axial dispersion coefficients for silica in FT-300 wax are similar to those for iron oxide up to a gas velocity of 0.04 m/s, thereafter the values for silica are higher than those for iron oxide. In general, it may be stated that the axial dispersion coefficient is independent of the type of liquid medium, and is only slightly affected by the type of solids used.

Wax and solids inventories

Wax and solids inventories (when solids were used) were made at the end of each run. The phase hold-up profiles in the column, storage tank level and solids concentrations, and weight of slurry samples withdrawn, were taken into consideration while making the inventory. In general, wax inventories showed better closures than did solids inventories, indicating some problems with solids settling.

In the run with small iron oxide, about 20% of the solids were unaccounted for during the run, while less than 2% of the wax was unaccounted for. Most of the settling occurred in the zone just above the distributor, and in the expansion unit above the column. In runs with large particles (iron oxide and silica), unaccounted solids ranged between 10 and 45%; however, in most cases the loss was due to a low concentration in the storage tank than in the column itself. The problem was particularly severe during continuous mode of operation at low liquid velocities (0.005 m/s). The solids settled in the overflow section, partially blocking the overflow line. The lines were cleared by temporarily increasing the liquid circulation velocity. Despite the problems with solids unaccountability, we were able to maintain solids concentrations in the column which averaged about 15-20 wt% when the expected value was 20 wt.%. At the end of a series of runs with a given batch of wax, accumulated wax and solids from the system were collected and it was found that the closures were always within 3% of the amount charged.

A.3. Average Gas Hold-up Correlations

Average gas hold-up data obtained from earlier runs conducted in the small (0.05 m ID) stainless steel column were used to establish gas hold-up correlations. Several correlations from literature were evaluated. We also used the drift flux approach to correlate our data. In addition to three-phase correlations, several two-phase correlations were also examined. For these correlations, slurry physical properties were used in place of liquid properties. While evaluating these correlations, we discarded hold-up data obtained in the presence of foam. This was done because these hold-up values are strongly influenced by the amount of foam, and the amount of foam produced at a given gas velocity is uncertain, i.e., reproducibility in the presence of foam is generally poor.

The correlations were evaluated using NLIN on SAS (non-linear regression) and in most cases the convergence criterion was met within 25 iterations. Between 50 and 75 data points were used in the analysis. The constants in the various correlations were reevaluated to minimize the mean squared error. Table 2 summarizes the resulting correlations, the corresponding mean squared errors and the literature reference from which the correlations were obtained. Except for the first correlation shown in Table 2, the mean square error for the other correlations was less than 0.0004. In all cases, measured hold-up values were within ±15% of hold-up values predicted by the correlations. We plan to update these correlations once additional data are available from the small (0.05 m ID) and the large (0.23 m ID) columns.

B. Task 4 – Application of a Gamma Radiation Density Gauge for Determining Hydrodynamic Parameters

During the experiments conducted in the last quarter, we also used the Cesium-137 density gauge to determine slug frequencies and flow regime transitions. The density gauge was placed at a fixed location for all runs, i.e. at a height of 1.5 m above the distributor. The signal from the gauge was recorded on the PC using the Metrabyte data acquisition system. We also recorded pressure fluctuations from the five pressure transducers located along the column height. However, time series analysis of data obtained from the pressure transducers indicated that a significant amount of damping of the fluctuations occurred probably because of partial blockage of the pressure ports with the large solid particles used in most of the experiments. We therefore used the pressure transducers to only obtain static pressures that were used to estimate axial and average hold-up values. Fluctuating signals obtained with the density gauge at every gas velocity for each run were analyzed and frequency spectra, histograms, and autocorrelations were estimated.

Figure 10 shows raw data obtained from the density gauge during the batch run with FT-300 wax in the absence of solids. The data were obtained at gas velocities of 0.02 m/s (Figure 10a) and at 0.06 m/s (Figure 10b). The large peaks in each figure correspond to the passage of large bubbles across the beam path of the density gauge. The regularity of these large peaks is significantly different at the two gas velocities. At 0.02 m/s, the large peaks appear randomly and also are less frequent; however, at 0.06 m/s, they appear at an increased regularity, and also have a relatively higher intensity (amplitude) than those at 0.02 m/s. This regularity indicates the presence of slugs in the dispersion at the gas velocity of 0.06 m/s. At the lower gas velocity (0.02 m/s), the bubbles are smaller and are randomly dispersed in the flow field. Additionally, the lower amplitude of the oscillations at this gas velocity is indicative of the larger liquid

fraction at 0.02 m/s relative to that at 0.06 m/s.

The power spectra for the signals obtained from the batch run with FT-300 (without solids) are shown in Figure 11 for gas velocities of 0.02, 0.04, 0.06, and 0.09 m/s. The four plots at the four different gas velocities clearly indicate the progressive movement of the dominant frequency to the left (towards lower values) with an increase in gas velocity. These results also show that the spectra are narrower at higher gas velocities (0.06 and 0.09 m/s) than they are at the lower gas velocities. This behavior in the frequency spectrum is indicative of the change in the flow regime in the bubble column. At low gas velocities, the homogeneous flow regime prevails and goes through a transition before approaching the slug flow regime at a gas velocity of about 0.06 m/s. The dominant frequency at a gas velocity of 0.02 m/s is in the range 7.5-10 Hz, and shifts to the range 2.5-5 Hz at 0.04 m/s, and finally approaches 2.5 Hz as slug flow develops at 0.06 m/s.

The probability density functions for the same data were also obtained and are shown in Figure 12 for the four gas velocities employed. The distribution at a gas velocity of 0.02 m/s has the shape of a normal distribution and can be associated with the homogeneous bubbly flow regime. However, as gas velocity is increased, the Gaussian distribution gets skewed to the right (e.g., at 0.04 m/s). At a gas velocity of 0.06 m/s, the formation of a second peak is evident at the right hand end of the distribution, which is more evident at 0.09 m/s. The second, smaller peak represents the fluctuations caused by the passage of slugs through the dispersion.

Results from other experiments with and without solids, and with Sasol wax are qualitatively similar to those observed with FT-300 wax. The transition to slug flow always occurred at about a gas velocity of 0.04 m/s, and the slug frequency was ~2.5 Hz at a gas velocity of 0.09 m/s for all runs.

V. Nomenclature

Ar	Archimedes number $= \frac{g d_p^3 \rho_\ell (\rho_p - \rho_\ell)}{\mu_\ell^2}$
C_s	solids concentration, g/cm^3
C_s^B	solids concentration at the bottom of the dispersion, g/cm^3
d_p	particle diameter, cm
d_{col}	column diameter, m
E_s	axial dispersion coefficient, cm^2/s
Fr	Froude number $= \frac{u_g}{\sqrt{g d_{col}}}$
Fr_t	Froude number $= \frac{(u_g + u_\ell)^2}{g d_{col}}$
Re_g	Reynolds number $= \frac{d_{col} u_g \rho_g}{\mu_g}$
$Re_{s\ell}$	Reynolds number $= \frac{d_{col}(u_g + u_\ell)\rho_{s\ell} g}{\mu_{s\ell}}$
t	time, s
u_g, U_g	superficial gas velocity, m/s
u_ℓ	superficial liquid velocity, m/s
U_p	hindered settling velocity of particles, m/s
U_T	terminal rise velocity of a single particle in an infinite medium, m/s

Greek letters

ϵ_g	gas phase hold-up
ϵ_ℓ	liquid phase hold-up
ϵ_s	solids phase hold-up
μ_ℓ	liquid viscosity, N.s/m
$\mu_{s\ell}$	slurry viscosity, N.s/m
ρ_ℓ	liquid density (g/cm^3)
ρ_p	solids density (g/cm^3)

$\rho_{s\ell}$	slurry density (g/cm^3)
Φ_ℓ	volume fraction of liquid in the slurry
$\overline{\Phi_\ell}$	average volume fraction of liquid in the slurry

VI. References

Badgujar, M. N., A. Deimling, B. I. Morsi, and Y. T. Shah, "Solids distribution in a batch bubble column," Chem. Eng. Comm., 48, 127 (1986).

Hatate, Y., D. F. King, M. Migita, and A. Ikari, "Behavior of bubbles in a semi-cylindrical gas-solid fluidized bed," J. Chem. Eng. Japan, 18, 99 (1985).

Kara, S., B. Kelkar, Y. T. Shah, and N. Carr, "Hydrodynamics and axial mixing in a three-phase bubble column," Ind. Eng. Chem. Proc. Des. Dev., 21, 584 (1982).

Kato, Y., A. Nishiwaki, T. Fukuda, and S. Tanaka, "The behavior of suspended solid particles and liquid in bubble columns," J. Chem. Eng. Jap., 5, 112 (1972).

Zheng, C., B. Yao, and Y. Feng, "Flow regime identification and gas hold-up of three-phase fluidized systems," Chem. Eng. Sci., 43, 2195 (1988).

Table 1. Conditions used during runs in the 0.05 m ID column[a]

Run No.	Wax type	Solids type	Solids size (μm)	Solids conc. (wt.%)	u_ℓ[b] (m/s)
S110-00000-2S	Sasol	none	–	–	0
S125-00000-2S	"	none	–	–	0.005
S135-FES20-2S	"	Iron oxide	0-5	20	0.005
S210-FEL20-2S	"	"	20-44	"	0
S225-FEL20-2S	"	"	"	"	0.005
F710-00000-2S	FT-300	none	–	–	0
F725-00000-2S	"	none	–	–	0.005
F730-FEL20-2S	"	Iron oxide	20-44	20	0
F742-FEL20-2S	"	"	"	"	0.02
F755-FEL20-2S	"	"	"	"	0.005
F810-SIL20-2S	"	Silica	"	"	0

[a]superficial gas velocities of 0.02, 0.04, 0.06 and 0.09 m/s were used in all runs
[b]superficial liquid velocity

Table 2. Summary of correlations used to fit average gas hold-up data

Correlation	MSE[a]	Reference
$\frac{u_g}{\epsilon_g} - \frac{u_\ell}{\epsilon_\ell} = 25.4\epsilon_g(1-\epsilon_g)^{-0.71}$	0.3867	Kara et al., 1982[b]
$\epsilon_g = 0.114 Fr^{0.35} Ar^{0.11}(1 + u_\ell / u_g)^{-0.48}(1-\epsilon_s)^{1.74}$	0.0002	Zheng et al., 1988
$\epsilon_g / (1-\epsilon_g) = 0.122 Fr^{0.46} Ar^{0.14}(1 + u_\ell / u_g)^{-0.65}(1-\epsilon_s)^{2.45}$	0.0002	Zheng et al., 1988[c]
$\epsilon_g = 0.048(1-C_s)^{0.37} u_g^{0.815}$	0.0003	Badgujar et al., 1986
$\epsilon_g = \frac{u_g/(u_g+u_\ell)}{0.92+0.33/\sqrt{Fr_t}}$	0.0004	Hatate et al., 1985
$\epsilon_g = \frac{u_g/(u_g+u_\ell)}{0.84+0.32/\sqrt{Fr_t}}(1-C_s)^{0.37}$	0.0004	Hatate et al., 1985[c]
$\epsilon_g = \frac{Re_g}{261+0.87Re_g+0.11Re_{sl}+635\left(\frac{\epsilon_s}{\epsilon_s+\epsilon_\ell}\right)}$	0.0001	Kara et al., 1982

[a]Mean squared error
[b]based on the drift flux approach
[c]modified form of the original correlation used

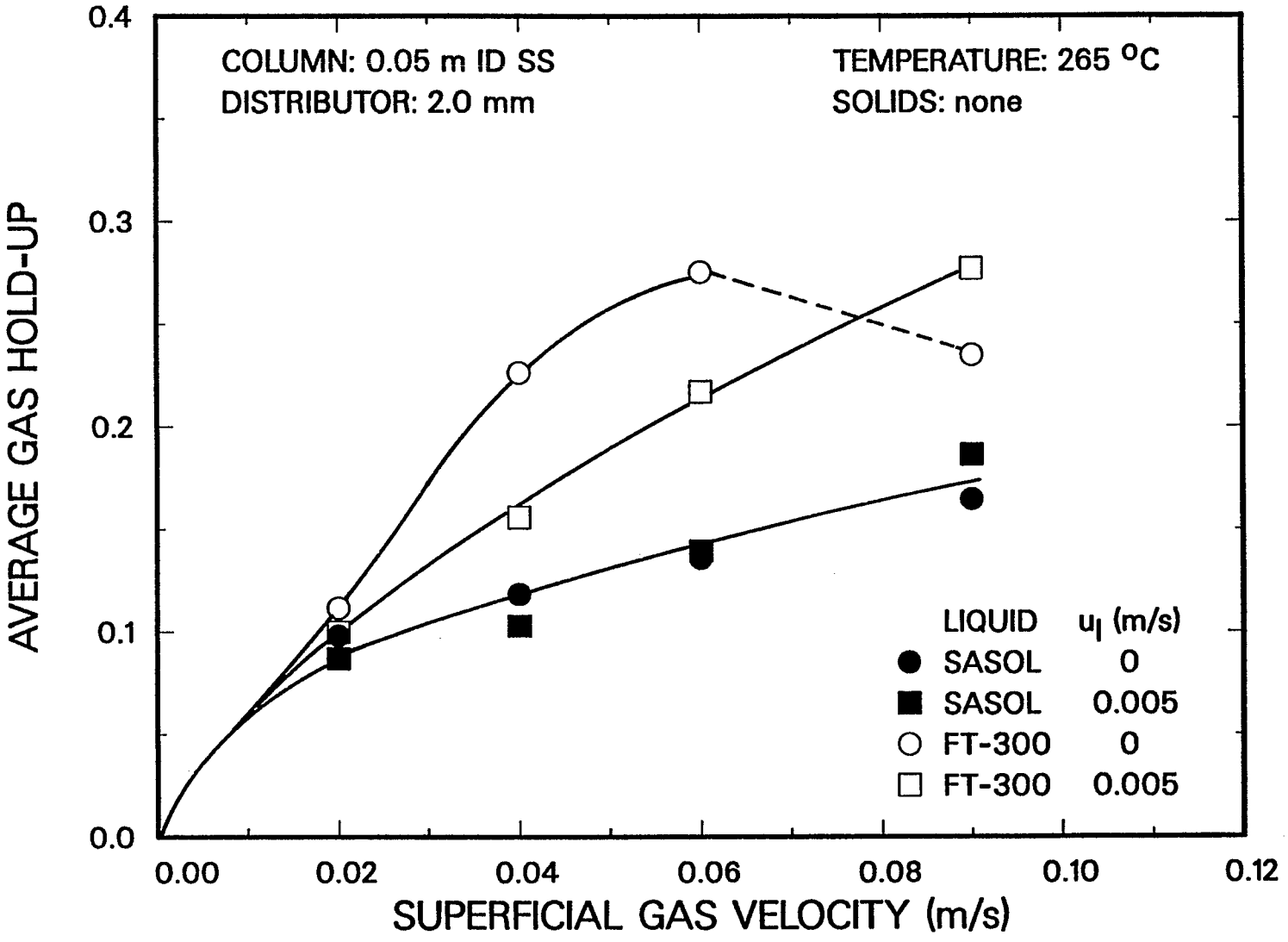

Figure 1. Effect of liquid type and liquid circulation velocity on average gas hold-up in the absence of solids.

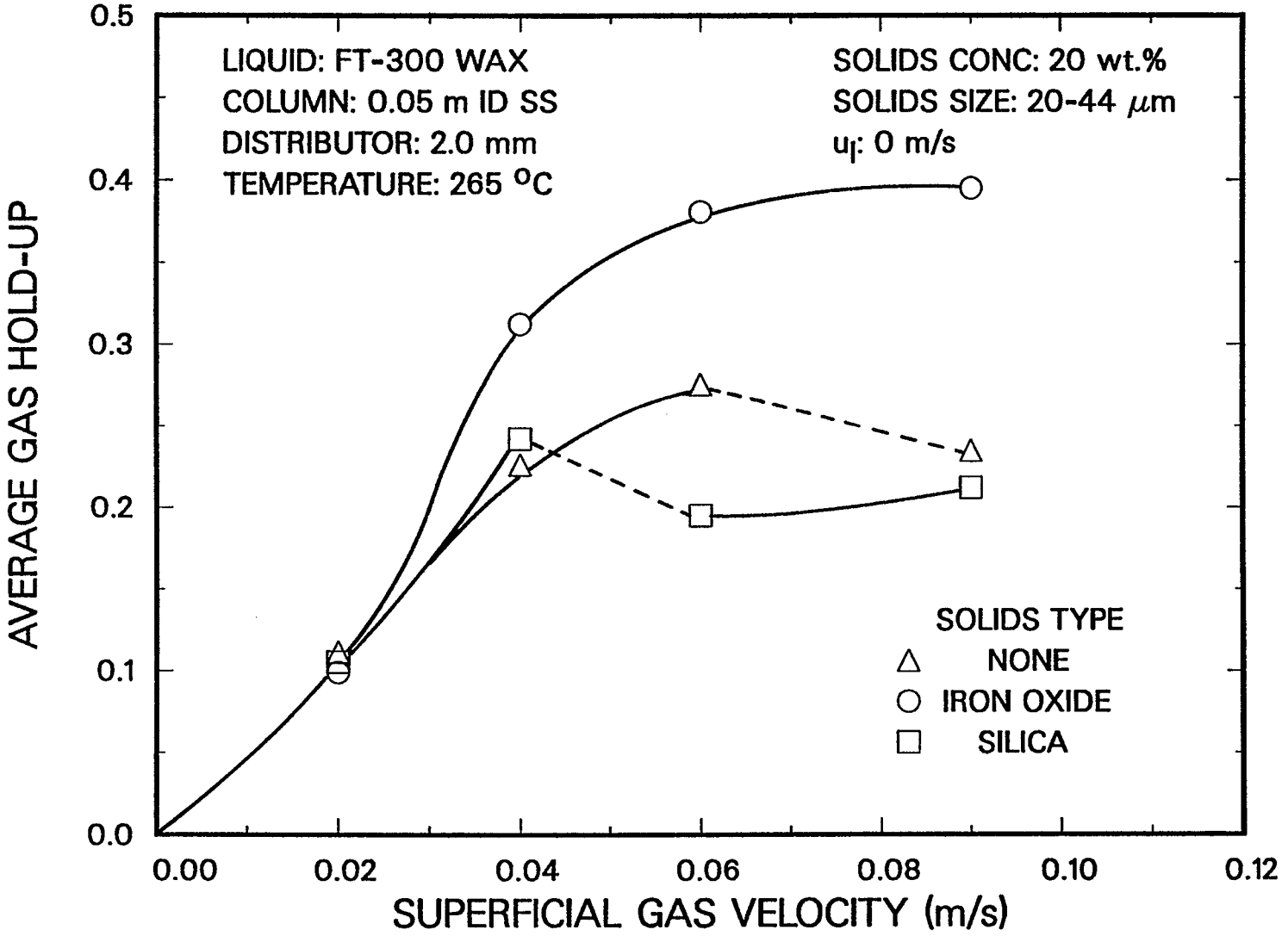

Figure 2. Effect of solids type on average gas hold-up.

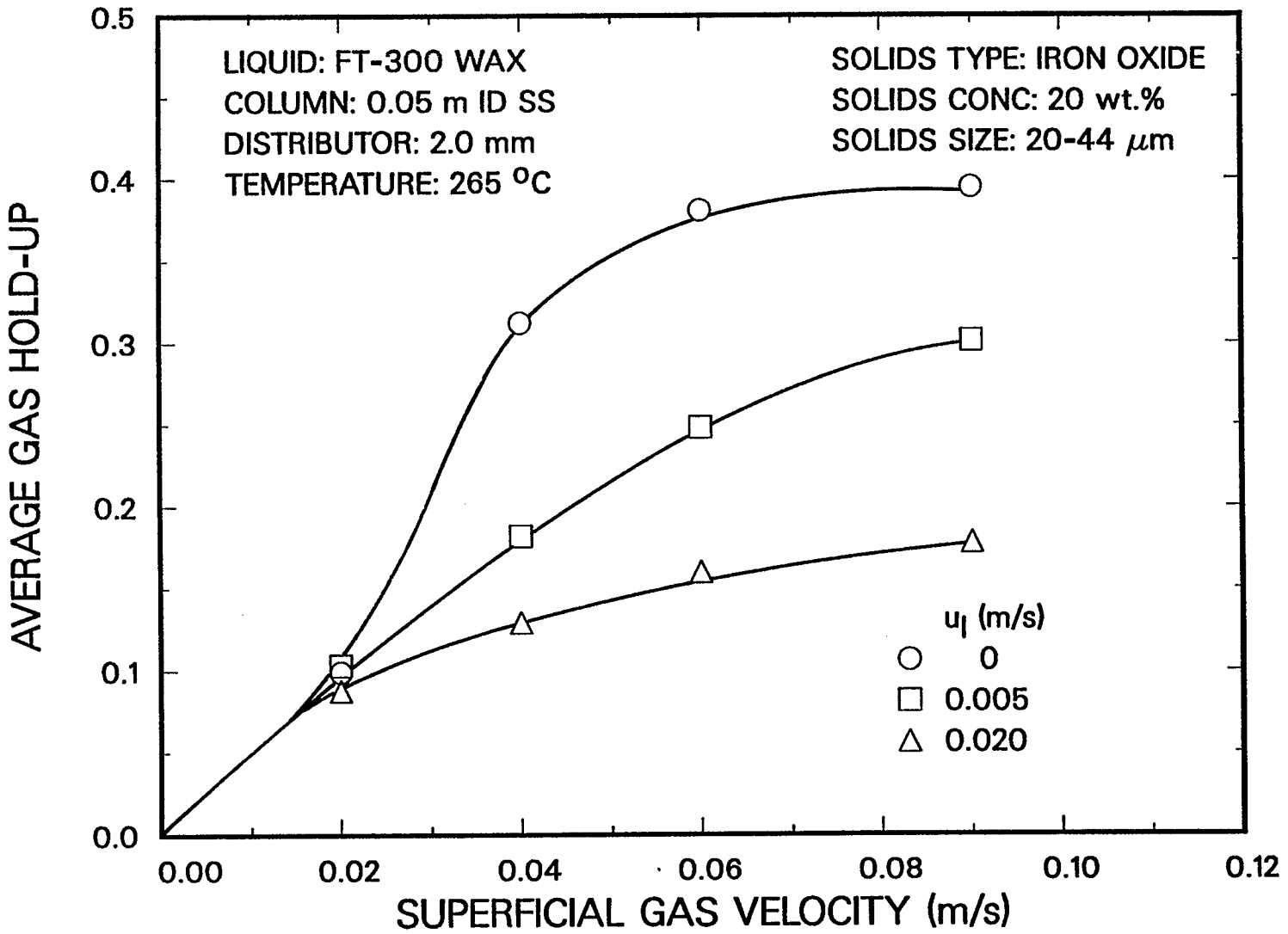

Figure 3. Effect of liquid circulation velocity on average gas hold-up in the presence of solids.

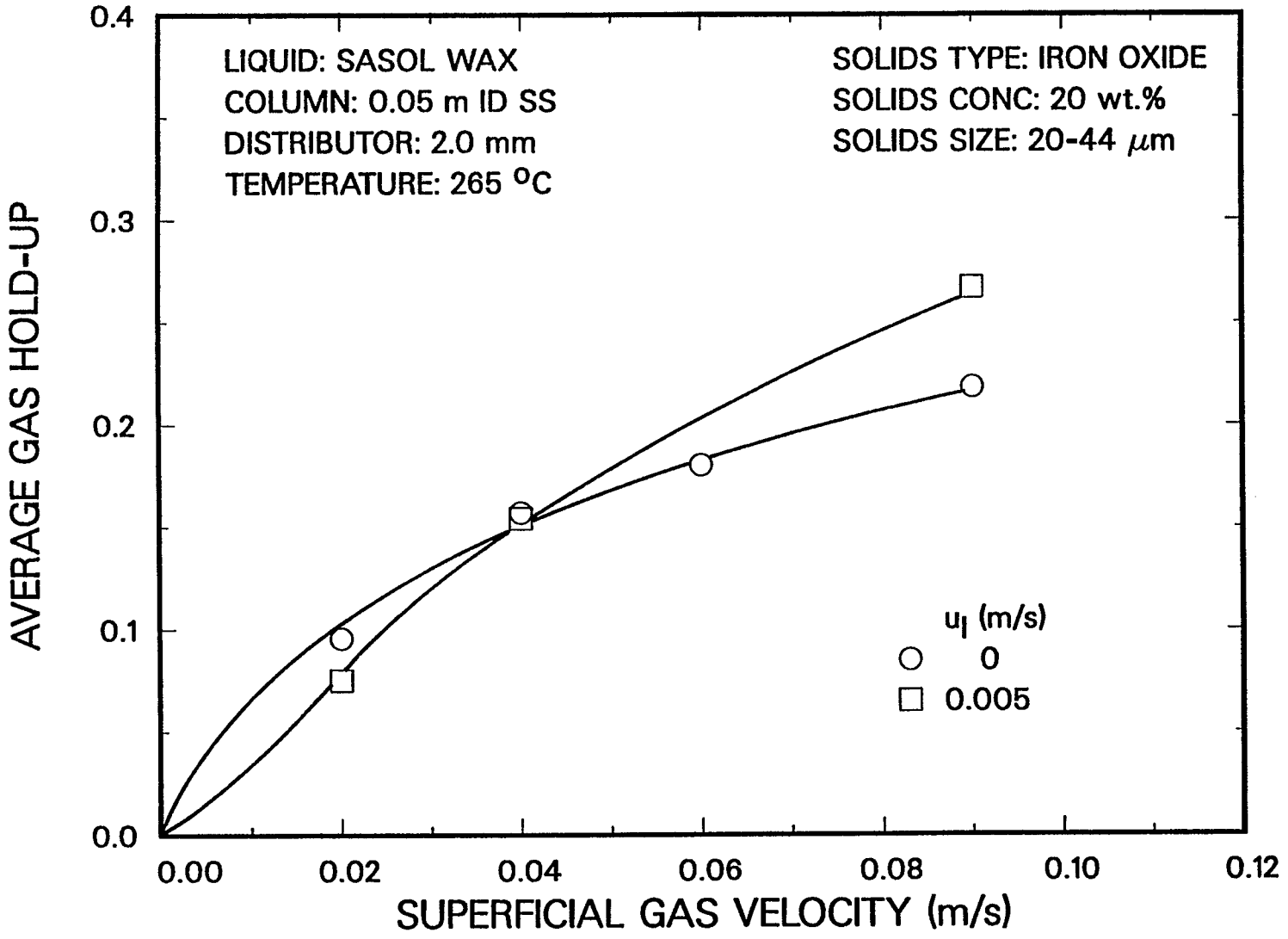

Figure 4. Effect of liquid circulation velocity on average gas hold-up in the presence of solids.

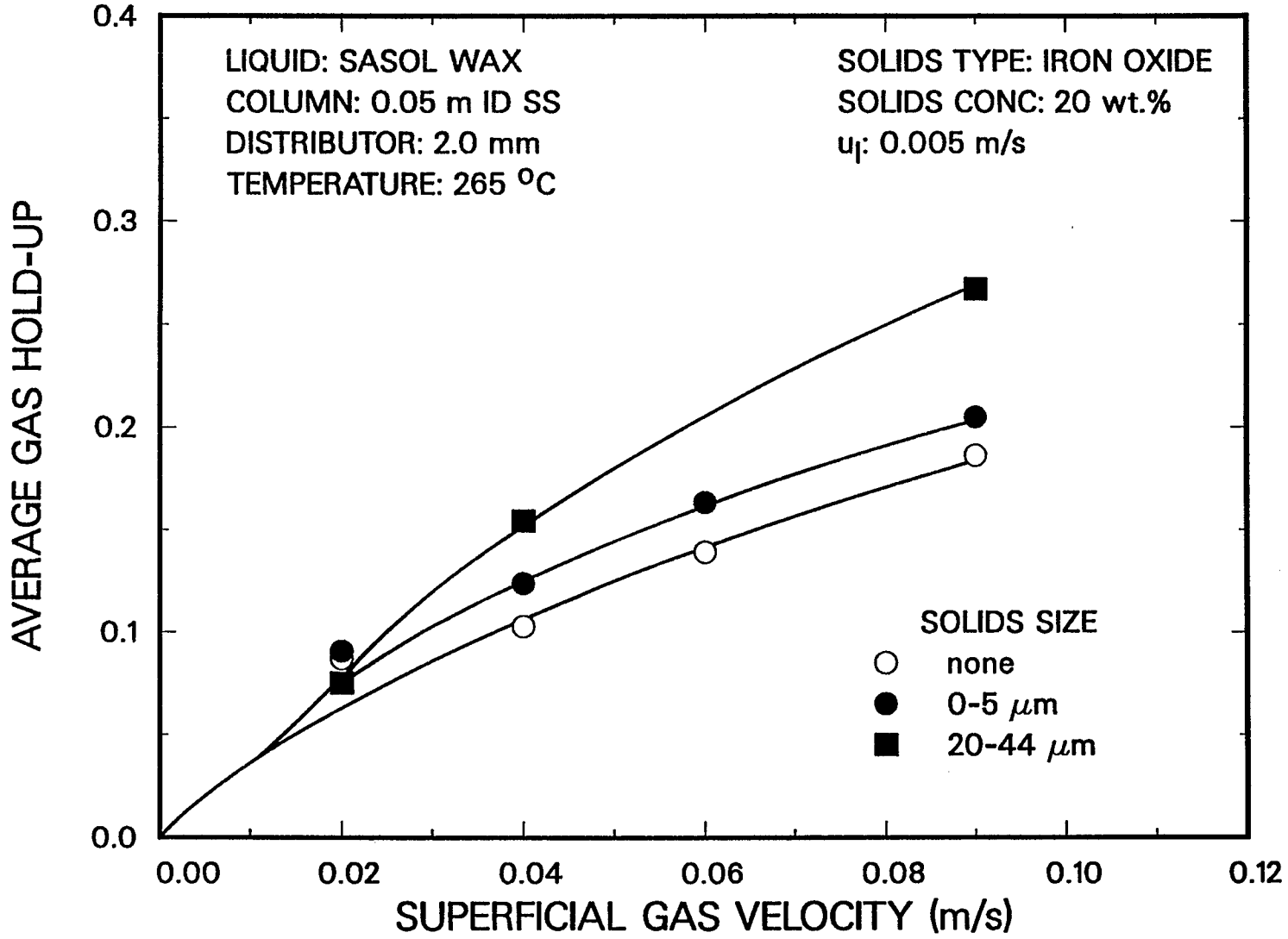

Figure 5. Effect of particle size on average gas hold-up.

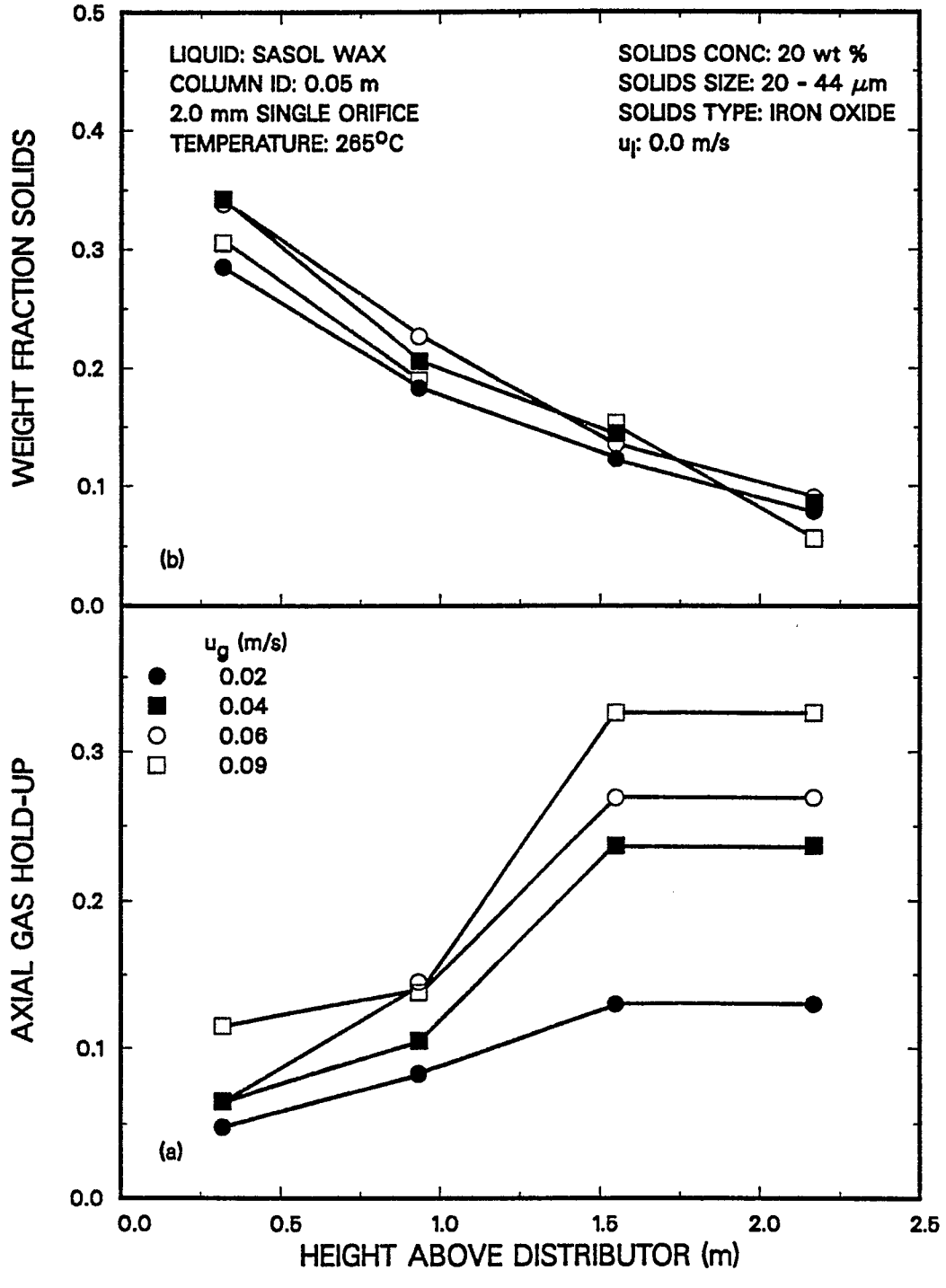

Figure 6. Effect of superficial gas velocity on (a) axial gas hold-up, and (b) axial solids distribution.

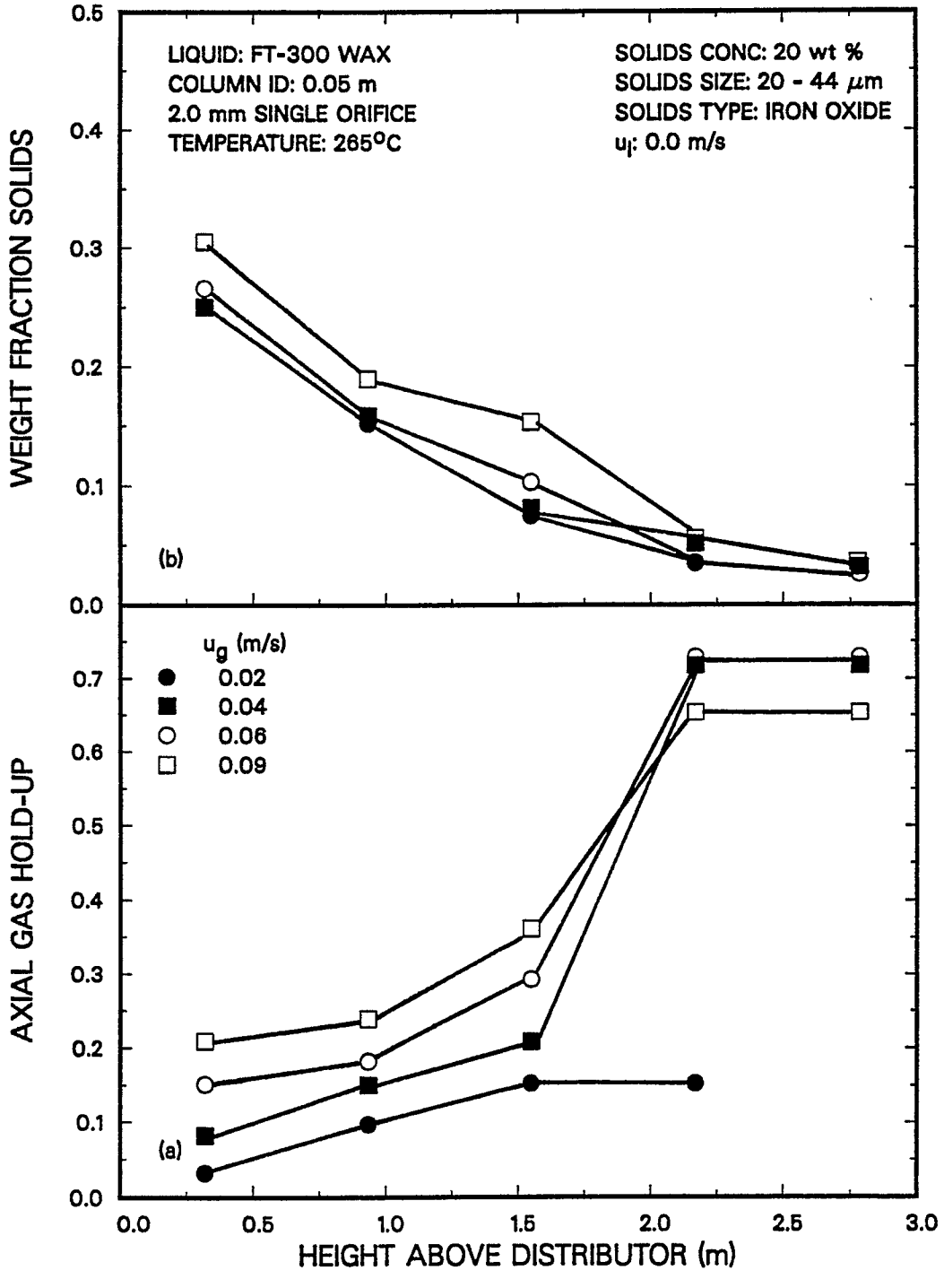

Figure 7. Effect of superficial gas velocity on (a) axial gas hold-up, and (b) axial solids distribution.

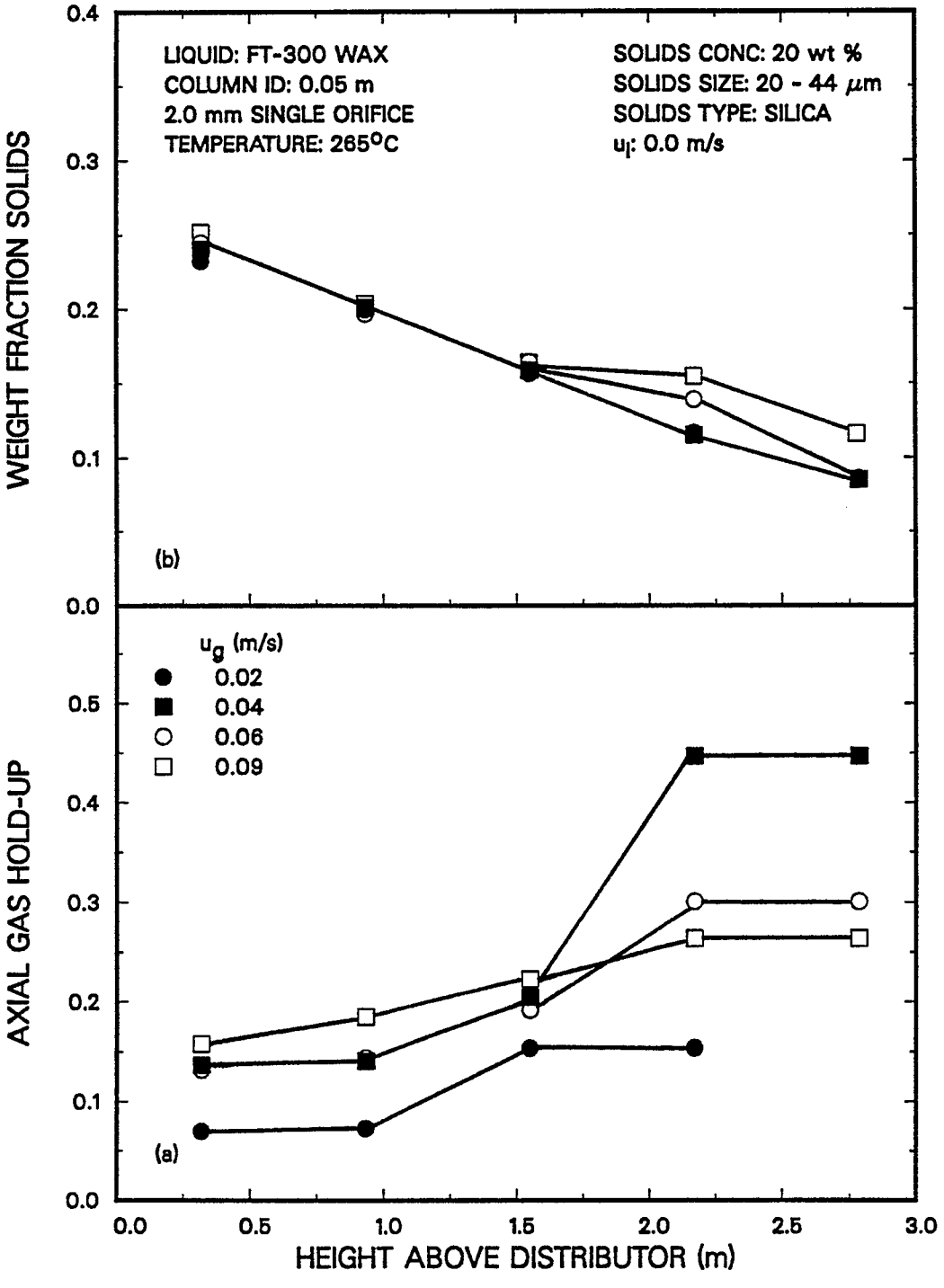

Figure 8. Effect of superficial gas velocity on (a) axial gas hold-up, and (b) axial solids distribution.

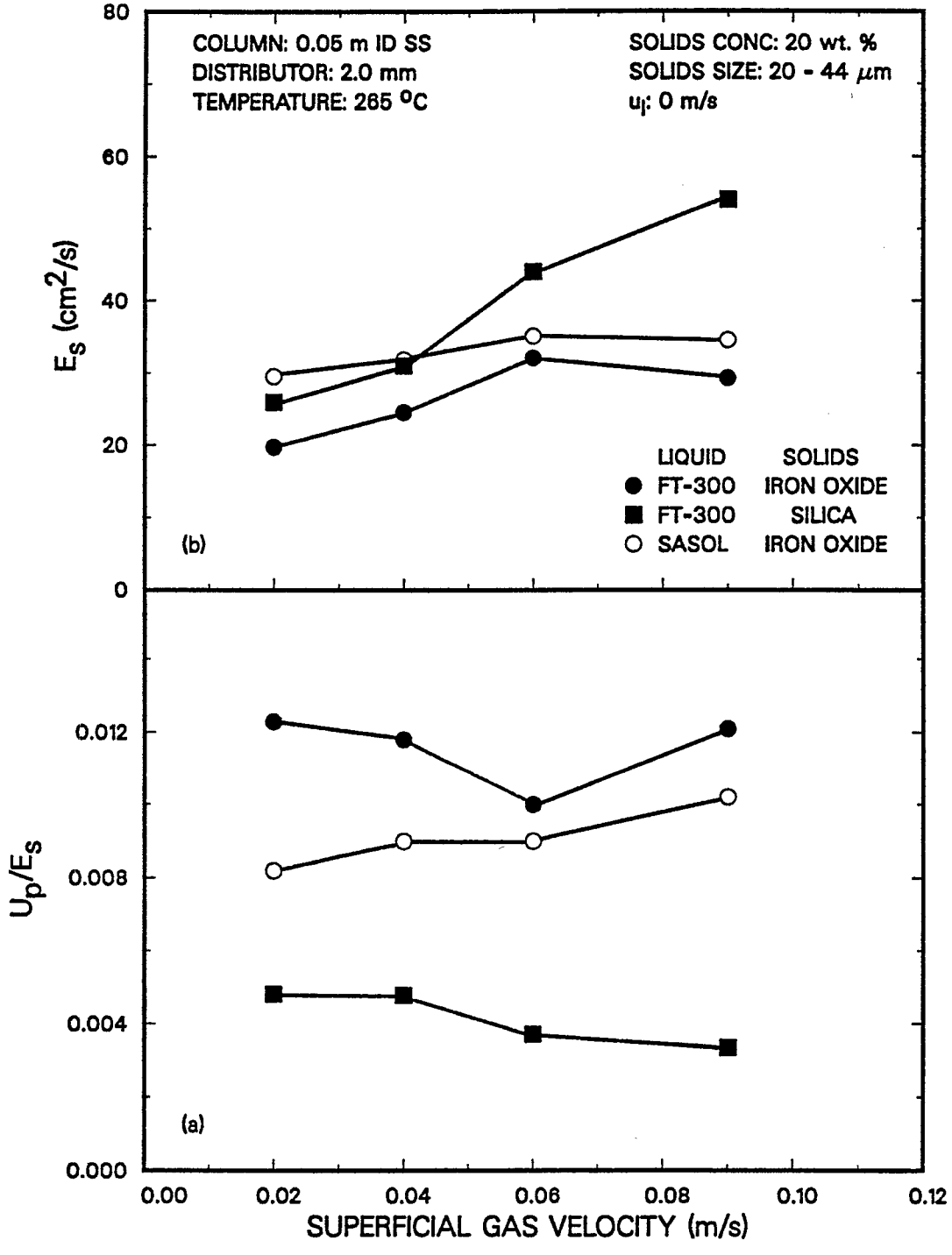

Figure 9. Effect of liquid medium and solids type on (a) Up/Es, and (b) axial dispersion coefficient.

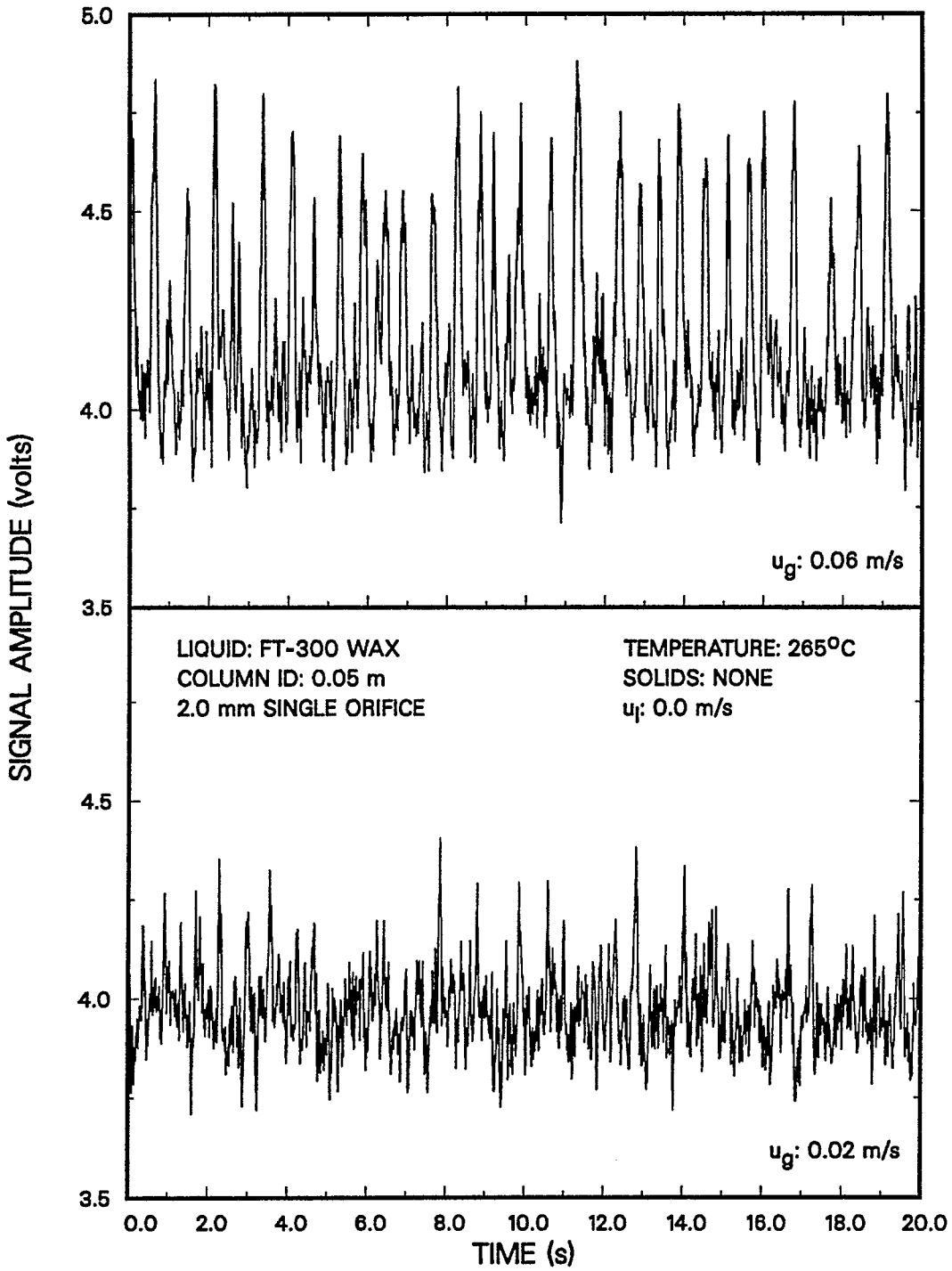

Figure 10. Typical raw signals from the nuclear density gauge apparatus using the Cesium-137 source.

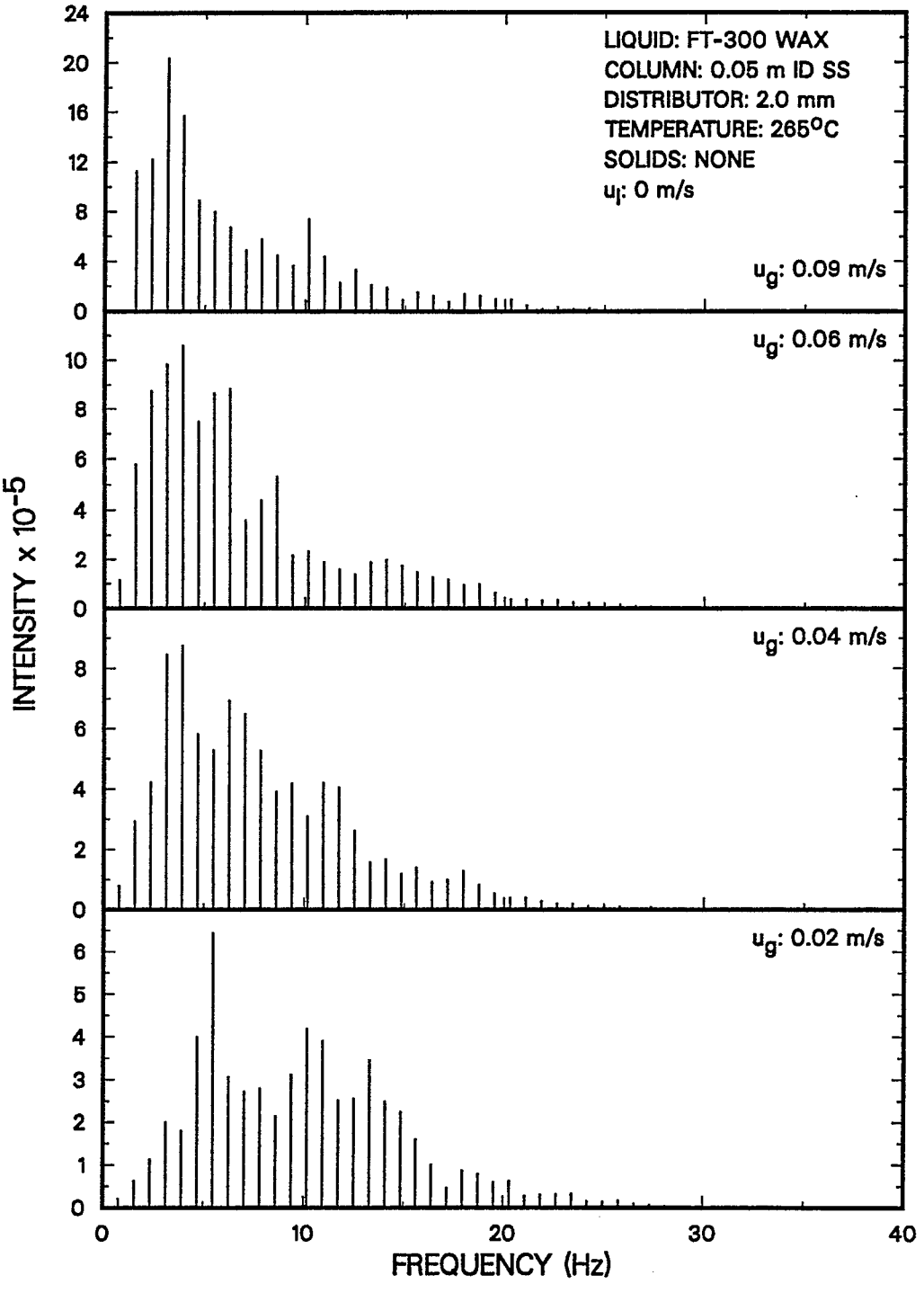

Figure 11. Effect of superficial gas velocity on the power spectral density function from the nuclear density gauge using the Cesium-137 source.

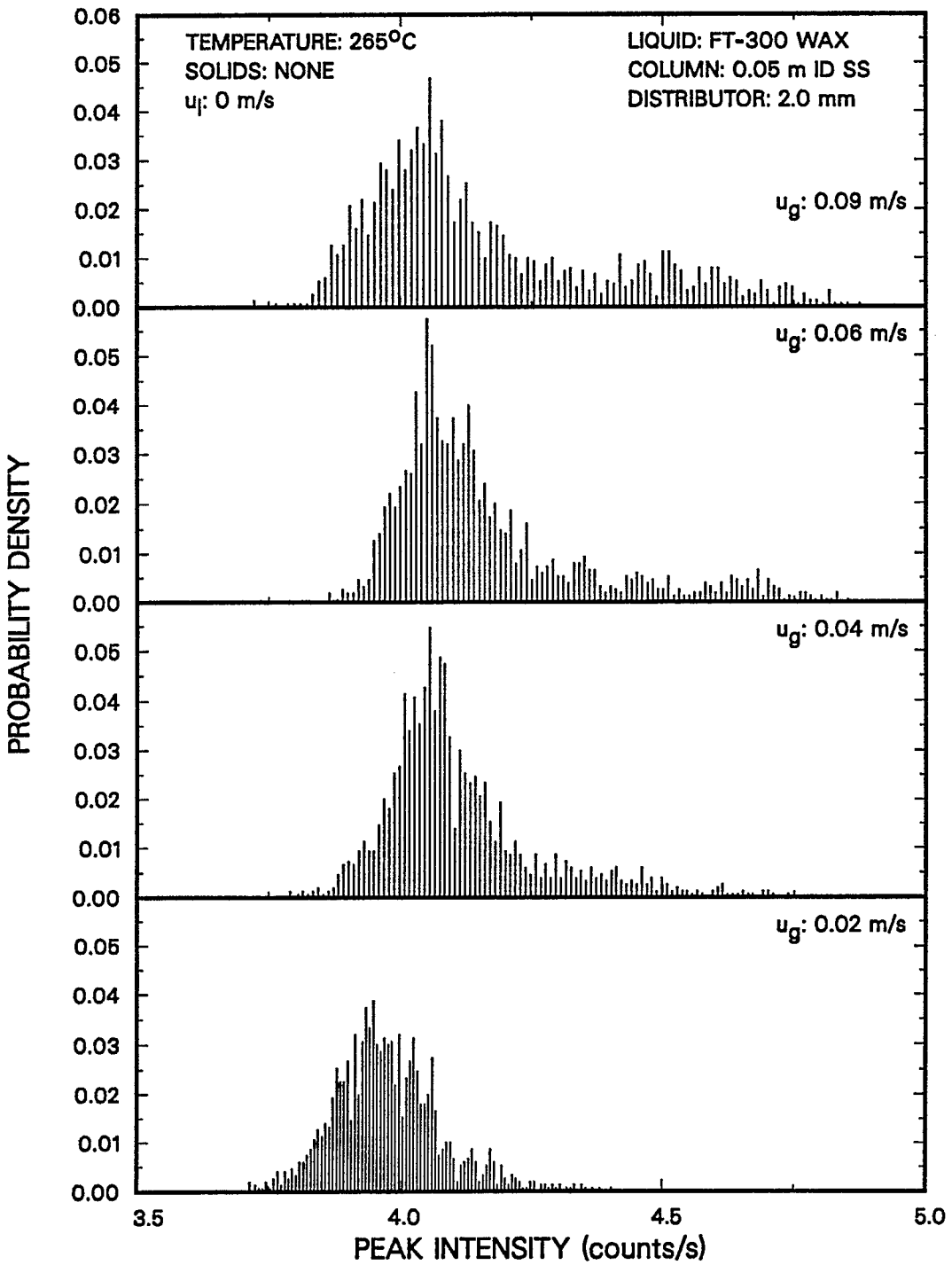

Figure 12. Effect of superficial gas velocity on the probability density function from the nuclear density gauge using the Cesium-137 source.